Transformation of the Sea-Ice "Cover" in the New Arctic — Insights Into Melt Progression From ICESat-2 High-Resolution Data Analysis With the DDA-bifurcate-seaice

Ute Herzfeld[1],
Thomas Trantow[1], Huilin Han[1], Adam Hayes[1], Ellen Buckley[2,3], Sinéad Farrell[3], Matthew Lawson[1], Nathan Kurtz[4], Thomas Neumann[4,5], Rachel Tilling[3,4], Marco Bagnardi[4], Michelle Hofton[3,5], Bryan Blair[3,5], Kutalmis Saylam[6]

(1) Geomathematics, Remote Sensing and Cryospheric Sciences Laboratory, Department of Electrical, Computer and Energy Engineering, University of Colorado at Boulder
(2) Brown University, (3) University of Maryland, (4) ICESat-2 Project, NASA Goddard Space Flight Center, (5) NASA Goddard Space Flight Center, (6) University of Texas at Austin

AGU Fall Meeting
Chicago and virtual
December 12-16, 2022

Importance of Observations on Melt Pond Evolution

- Arctic sea ice has been reported to reach historic lows repeatedly
- Transition from a perennial to a seasonal Arctic sea-ice cover is imminent
- Melt ponding is a key process
- Predictions based on models diverge
- Melt pond evolution is a complex process and needs observations
- NASA's ICESat-2 captures melt ponds (in the photon point cloud)

Perovitch et al. 2002, 2003, Stroeve et al. 2007, 2012, 2018, Serreze et al., 2007, 2008, Tschudi et al. 2008, Markus et al. 2009, Petty et al. 2018, Kwok 2018, Scott and Feltham 2010, Jahn et al. 2011, Hunke et al. 2013, Holland et al. 2012, Perovich and Polashenski 2012, Polashenski et al. 2012, Notz et al. 2020, Shupe et al 2020, Rösel et al. 2012, Farrell et al. 2020, Tilling et al. 2020, Webster et al. 2015, 2022, Neumann et al. 2019, among other papers

ICESat-2 records melt ponds on sea ice in ATL03

... but not in the standard sea-ice products (ATL07, ATL10)

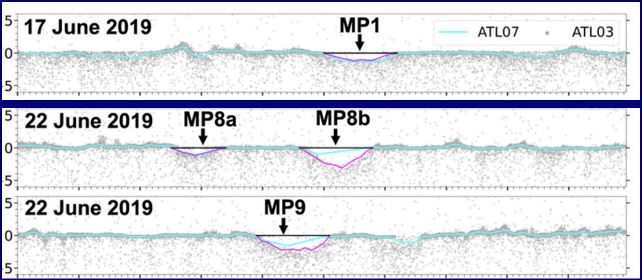

Detection of sea-ice melt ponds with ICESat-2 in the Lincoln Sea. ATL03 photon heights (gray), ATL07 height (cyan), and University-of-Maryland-MPA-derived melt pond (MP) surface (black) and bottom (magenta) elevations (After Farrell et al. 2020).

Automated Detection and Depth Determination of Melt-Ponds on Sea Ice Among Ridges and Smooth Surfaces: The DDA-bifurcate-seaice

A collaboration with Sinead Farrell and Ellen Buckley (U Maryland, EB: now Brown University)

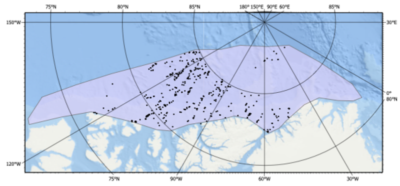

Multi-year Arctic sea-ice region (MYASIR) with pond locations, ≈ 500 ponds manually identified and computationally analyzed (UMD).

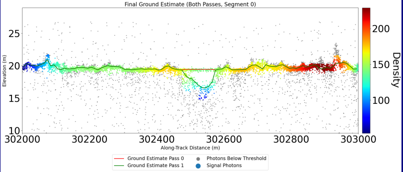

Automated pond detection and measurement with DDA-bif-seaice

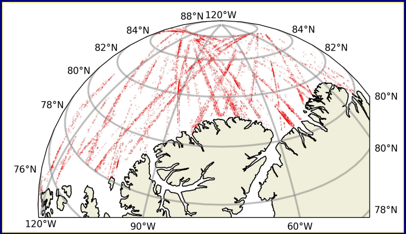

MYASIR with pond locations, ≈ 10200 ponds automatically detected and measured with DDA-bif-seaice. Processed on ADAPT.

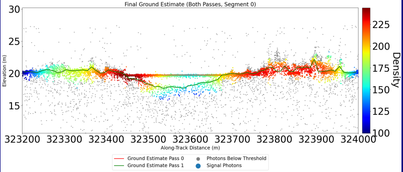

Herzfeld,Trantow, Han, Buckley, Farrell, Lawson, TGRS (subm.),

preprint doi:10.36227/techrxiv/21300153.v1 (October 2022);

see also Ellen's PhD Thesis and Buckley et al. (in prep.)

The ICESat-2 Advanced Topographic Laser Altimeter System (ATLAS)

- Launch Sept 12, 2018
- First space-borne multi-beam micro-pulse photon-counting laser altimeter system
- Wavelength 532nm (green)
- Pulse-repetition frequency 10 kHz
- Multi-beam: 3 sets of {strong beam, weak beam}, separated by 90 m, with 3 km separation to the next set of beams
- Field of View: 40 m, footprint 17 m diameter
- Along-track spacing: 0.7m
- Orbit altitude: 496 km
- Orbit inclination: 92°
- 91-day repeat cycle
- Orbit determination: High-precision GPS and laser ranging
- Attitude determination: star tracker
- Airborne simulator instruments: Multiple Altimeter Beam Experimental Lidar (MABEL) and Slope Imaging Multi-polarization Photon-counting Lidar (SIMPL)
- ICESat-2 data products are available under https://earthdata.nasa.gov/

The Density-Dimension Family of Algorithms

Algorithms

- DDA-atmos: Official algorithm for atmospheric data products (ATL09): clouds, aerosols, blowing snow, diamond dust
- DDA-ice-1: Ice-surfaces (glaciers, crevassed regions; all surfaces)
- DDA-ice-2: Ice surfaces with secondary surfaces
- DDA-bifurcate-seaice: Melt ponds on sea ice, also non-bifurcating sea-ice surfaces, including ridges
- DDA-bifurcate: Any bifurcating surfaces (melt ponds in Greenland, on ice shelves, shallow-water bathymetry)

Algorithm Properties

- Input: ATL03 photon point cloud
- High resolution of surfaces and ponds (smallest detected ponds: 7.5m diameter, depth resolution: 0.2m)
- The DDA is an auto-adaptive algorithm (adapts to background, daylight/night conditions, ASR)
- DDA utilizes core math of a neural net (the radial basis function) in a new way: runs efficiently

Herzfeld et al. TGRS, 2017 (doi:10.1109/TGRS.2016.2617323); Herzfeld et al. Science of Remote Sensing, 2021 (doi:10.1016/j.srs.2020.100013); H. et al. GRL 2021 (doi:10.1029/2021GL093473); H. et al. ATBD atmos 2021 (release 5 data; doi:10.5067/48PJ5OUJOP4C); H et al. Remote Sensing 2022 (doi: 10.3390/rs14051185); H et al. TGRS (2022 subm, see doi:10.36227/techrxiv/21300153.v1)

Steps of the DDA-bifurcate-seaice

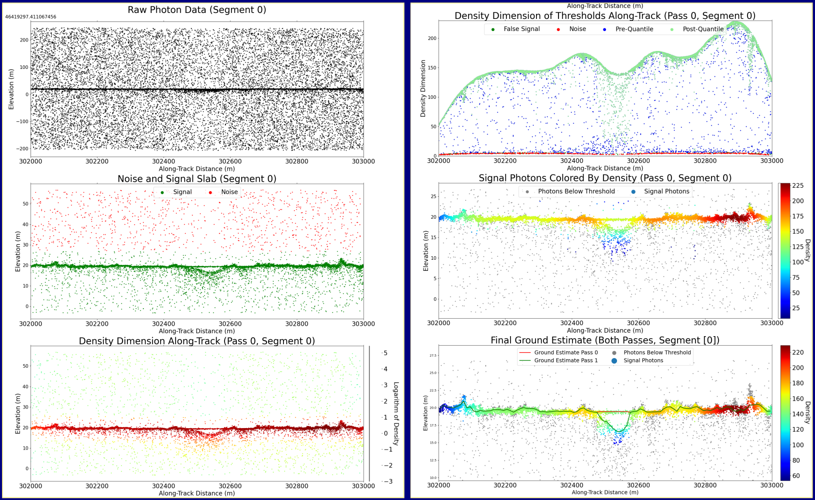

1298_gt3l_82.637.png [mega 1], Data from the Lincoln sea, ICESat-2 ATLAS granule

ATL03_20190622061415_12980304_005_01.h5, RGT 1298, collected 2019-June-22, ICESat-2 ASAS version 5 data.

[from Herzfeld et al. IEEE TGRS 2022 (subm. Oct. 2022), see: doi:10.36227/techrxiv/21300153.v1]

Comparison of Results:

ATL07 – UMD melt-pond algorithm (MPA) – DDA-bif-seaice

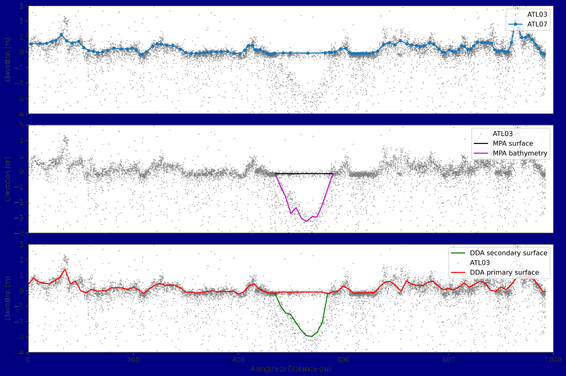

2019 data: 1298_gt3l_82.637

[from Herzfeld et al. IEEE TGRS 2022 (subm. Oct. 2022), see: doi:10.36227/techrxiv/21300153.v1]

DDA-bif-seaice Pond Examples – Summer 2019 ICESat-2 ATLAS data – Lincoln Sea

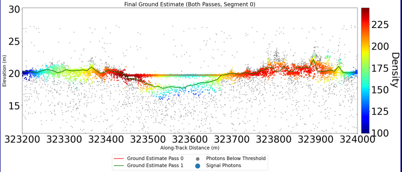

(a) 1237_gt3l_82.818.png [mega 3]

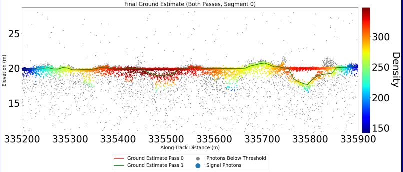

(b) 1237_gt1l_82.906.png

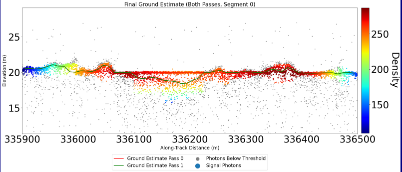

(c) 1237_gt1l_82.906_2.png

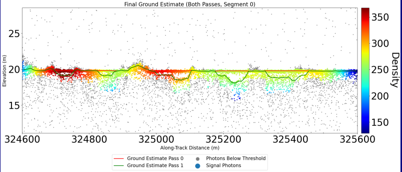

(d) 1237_gt3l_82.831.png [mega 4]

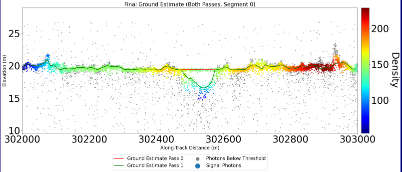

(e) 1298_gt3l_82.637.png [mega 1]

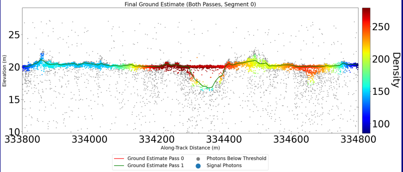

(f) 1298_gt3l_82.911.png [mega 2]

DDA-bif-seaice Pond Examples – Summer 2020 ICESat-2 ATLAS data – Lincoln Sea

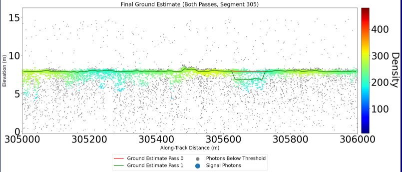

(a) 2020data/0713, seg305

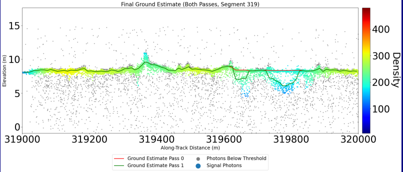

(b) 2020data/0713, seg319

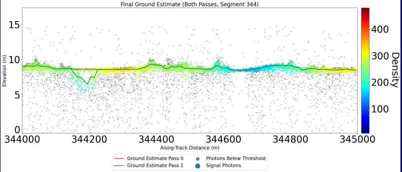

(c) 2020data/0713, seg344

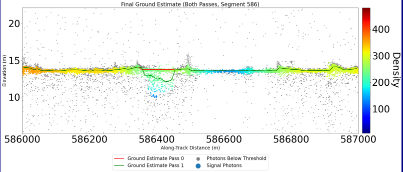

(d) 2020data/0713, seg586

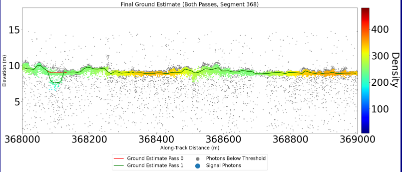

(e) 2020data/0713, seg368

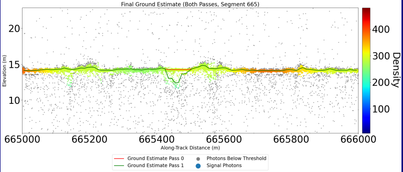

(f) 2020data/0713, seg665

Saturation Problem – Summer 2020 ICESat-2 ATLAS data – Lincoln Sea

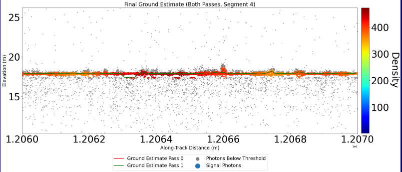

(a) 2020data/0803, seg4

(a false pond)

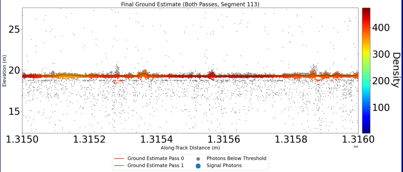

(b) 2020data/0803, seg113

(dead-time effect artifacts avoided)

Examples of ponds are from ICESat-2 ATLAS granule 20200803013027_05910804_005_01 gt1l strong outer beam, reference ground track (RGT) 591, collected 2020-August-3, ICESat-2 ASAS version 5 data set.

[from Herzfeld et al. IEEE TGRS 2022 (subm. Oct. 2022), see: doi:10.36227/techrxiv/21300153.v1]

Towards Implementation of Melt-Pond Information on the ICESat-2 Sea-Ice Products: Determination of Parameters and Variables of the DDA-bif-seaice Using Airborne Campaign Data

PI: Ute Herzfeld, University of Colorado Boulder

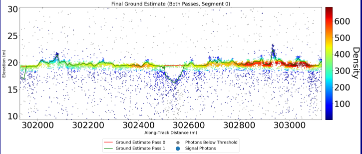

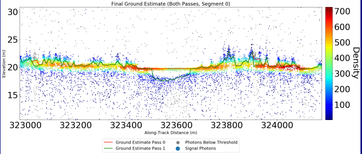

Automated detection of melt ponds on sea ice among ridges and smooth surfaces: The DDA-bifurcate-seaice.
ICESat-2 data from the Lincoln Sea (From Herzfeld, Trantow, Buckley, Farrell, Lawson (in prep.)).

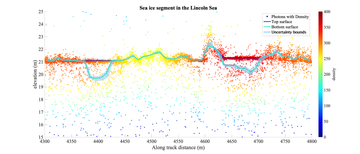

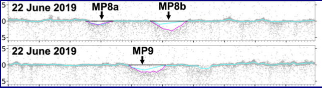

ATL07 misses ponds; and UMD algo (Farrell et al. 2020)

(1) Assessment of the feasibility for a melt pond depth recovery algorithm that could become part of the ICESat-2 standard data products

(2) Determination of parameters and variables of the DDA-bifurcate-seaice, to retrieve melt ponds and reduce uncertainties in determination of melt-pond depth

(3) Derivation of value-added reference data sets through analysis of the campaign data sets and ICESat-2 ATLAS data, in support of all three mission goals

(4) Analysis of all ICESat-2 ATLAS data from all tracks underflown by the Arctic sea-ice campaign and the PI's Svalbard data collection

(7) Mathematical description of the planned algorithm for melt-pond detection and melt-pond depth as part of the standard ICESat-2 data products

Summer 2022 ICESat-2 Arctic Sea-Ice Campaign

conducted by the ICESat-2 Project Science Office in July 2022 from Thule, Greenland

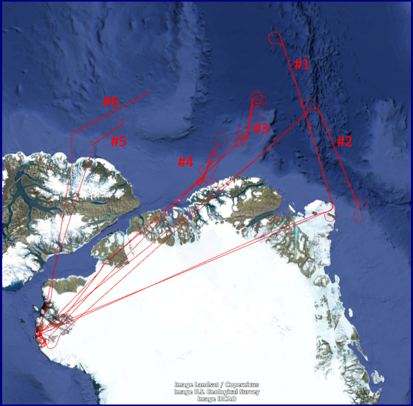

Flight paths (from Rachel Tilling and Marco Bagnardi)

- Collection of LVIS 1064 wide-swath imaging laser altimeter system data and hi-res imagery (Brian Blair, Michelle Hofton, NASA)
- and Chiroptera bi-color (NIR and green) laser altimeter data (Kutalmis Saylam, Economic Geology, University of Texas)

Summer 2022 ICESat-2 Arctic Sea-Ice Campaign

conducted by the ICESat-2 Project Science Office in July 2022 from Thule, Greenland

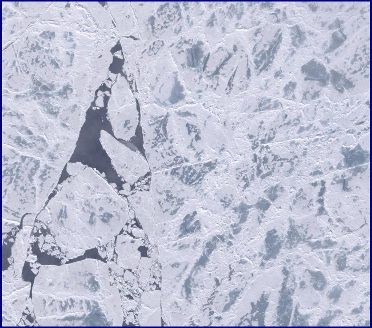

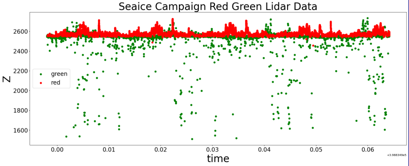

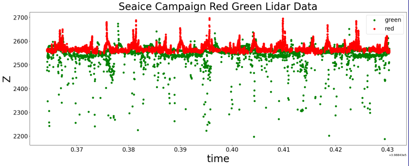

LVIS 1064 wide-swath imaging laser altimeter system and hi-res imagery
(Brian Blair, Michelle Hofton, NASA)
https://icesat-2.gsfc.nasa.gov/pages/lvis-phaseone-quicklook-georeferenced-imagery
(NASA ICESat-2 Project, Oct. 2022)
Blair, J. B., Hofton, M., Harbeck, J., and N. Kurtz 2022. LVIS L1B PhaseOne QuickLook Georeferenced Imagery, Version 1. Greenbelt, Maryland USA. NASA Goddard Space Flight Center.

Chiroptera bi-color (NIR and green) laser altimeter
(Kutalmis Saylam, Economic Geology, University of Texas)

[data sample with preliminary corrections:

https://utexas.box.com/s/88d4uyl3bx3xtvtw53y14pz08i6nd1uy

(NASA ICESat-2 Project, Nov. 2022),

plots by Huilin Han, Geomath lab, CU Boulder]

Airborne Validation of ICESat-2 Sea-Ice Observations and DDA-bifurcate-seaice Data Products in an Area of Ice-Ocean-Seaice Interaction in Svalbard (Summer 2023)

ICESat-2 validation campaign, Svalbard

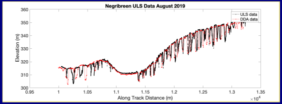

ICESat-2 DDA vali results (Herzfeld et al. 2022)

(5) Field work: Collection of ancillary data (high-resolution laser altimetry, imagery, GPS and IMU data) over ICESat-2 ground tracks over melt features on off-shore floating ice and land ice in the area of the Negribreen Glacier System (NGS), Svalbard, which, due to the current surge, is an area of heavy ice-ocean-interaction featuring highly fractured calved glacier ice, brash ice and sea ice, as well as water in/on complex ice surfaces on land [augmentation of funded NSF/NASA field work]

(6) Analysis of geophysical data from PI-led campaign and additional evaluation of ICESat-2 melt-pond recovery algorithm, augmentation of the value-added reference data sets

(7) Mathematical description of the planned algorithm for melt-pond detection and melt-pond depth as part of the standard ICESat-2 data products

(8) Publication and sharing of results and value-added data sets

ICESat-2 Airborne Validation Campaigns 2018-2019: NASA/NSF/SIOS

Combining observation of the surge with airborne evaluation of ICESat-2 data:

(a) Assessment of ICESat-2 ATLAS measurement capability over complex ice surfaces: crevasses, fractures, rifts, water on ice, firn, snow, bare ice

(b) Evaluation of ICESat-2 height determination (DDA-ice-1, ice-2) over crevassed and other complex terrain

(c) Kinematic and RTK GPS experiments (with UNAVCO)

(d) Special Acquisition of Planet SkySat Data (2019)

— A contribution to Svalbard Integrated Arctic Earth Observing System (SIOS)

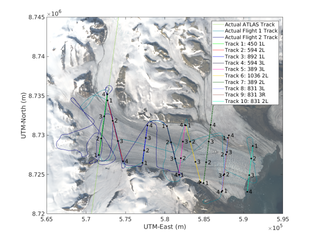

Flight 1, 2019-Aug-12; Flight 2: 2019-Aug-13
Landsat-8, 2019-08-05

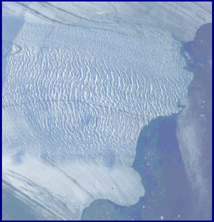

SkySat Image 2019-Aug-18

Field Team 2019

Experiment Setup:

(1) Laser altimetry (ULS (Lasertech), CU Geomath Integration)

(2) Time-laps imagery (Go-Pro Hero5)

(3) IMU Data (Attitude Correction)

(4) On-board Kinematic GPS

(5) GPS base station at Negri-edge

GPS Base Station 7/2018

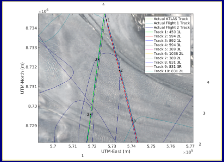

zoom RGT 450, 594

Negribreen ICESat-2 Validation Campaign 2019: Geodetical accuracy of airborne geophysical validation from a helicopter (after differential GPS and IMU correction)

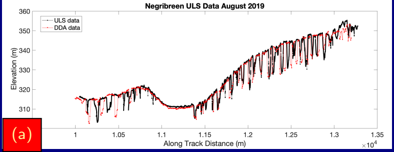

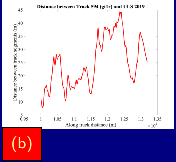

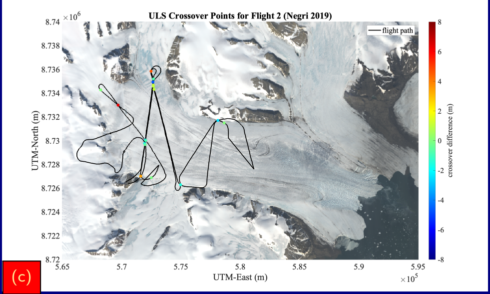

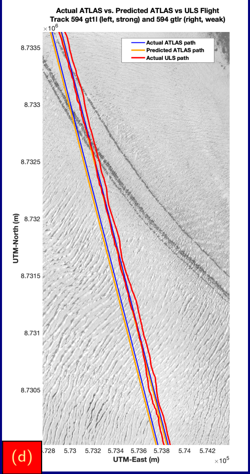

(a) ULS data (black) over DDA-processed ICESat-2 data (red) for a crevassed area along RGT 594. (b) Average distance of ULS and ICESat-2 tracks is 25m (for RGT450, 17m). (c) Crossover elevations for the flight in upper Negribreen 2019. There are 17 crossover locations with a mean difference of 0.0879±2.755 meters. Removing the six crossover points on large turns, the mean difference is 0.192±2.385 meters. (d) ICESat-2 and ULS ground tracks for RGT 594 (Herzfeld et al. 2022, doi:10.3390/rs14051185).

Conclusions

(1) ICESat-2 ATLAS data contain information on melt ponding

(2) DDA-bifurcate-seaice allows automated detection and depth measurement of melt ponds (without a-priori information on pond locations)

(3) Smallest detected ponds are 7.5m (along-track diameter), depth resolution 0.2m

(4) Processing on the NASA Cloud (ADAPT) finds 10000+ melt ponds in one summer season (in 10% of the data)

(5) Facilitates first study of evolution of melt ponds (Buckley et al. in prep)

(6) Evaluation using summer Arctic sea-ice campaign

(7) Goal: Implementation of the DDA-bifurcate-seaice as operational algorithm to provide pond info on the ICESat-2 seaice products

Acknowledgements: Work on ICESat-2 algorithm development, validation and science applications supported by NASA Earth Sciences and the ICESat-2 Project; research on Negribreen Surge also supported by NSF Arctic Natural Sciences. Research on image classification supported by NASA and NSF Cyberinfrastructure and ANS. A contribution to Svalbard Integrated Earth Observing System (SIOS), registered as Research in Svalbard Project RIS-10827 "Negribreen Surge" (2017-2019). 2018 campaign partly supported through a SIOS Access Pilot Project (2017_0010). Planet SkySat data collected under the NASA CSDAP.